Theoretical Insight into the Interactions of TMA-Benzene and TMA-Pyrrole with B3LYP Density-Functional Theory (DFT) and ab Initio Second Order Møller−Plesset Perturbation Theory (MP2) Calculations

Tong Liu,[†] Jiande Gu,*[,†] Xiao-Jian Tan,[†] Wei-Liang Zhu,[†,‡] Xiao-Min Luo,[†] Hua-Liang Jiang,*[,†] Ru-Yun Ji,[†] Kai-Xian Chen,[†] Israel Silman,[§] and Joel L Sussman*[,||]

Center for Drug Discovery & Design, State Key Laboratory of Drug Research, Shanghai Institute of Materia Medica, Shanghai Institutes for Biological Sciences, Chinese Academy of Sciences, 294 Taiyuan Road, Shanghai 200031, P. R. China, Chemical Process & Biotechnology Department, Singapore Polytechnic, 500 Dover Road, Singapore 139651, Department of Neurobiology, Weizmann Institute of Science, 76100 Rehovot, Israel, and Department of Structural Biology, Weizmann Institute of Science, 76100 Rehovot, Israel

Received: August 28, 2000; In Final Form: March 5, 2001

A detailed theoretical investigation of the tetramethylammonium(TMA)-benzene and TMA-pyrrole complexes has been performed to obtain the interaction properties of TMA with aromatics. Diffuse functions have been found to be important in the computational studies of these noncovalent complexes. Adding diffuse functions to the basis set decreases the binding energy by about 10% for the TMA-aromatic systems. Dispersion interactions in the TMA-aromatic systems are very important. They enhance the binding interactions between the TMA and the aromatic ring systems by about 0.5 kcal·mol^{-1} per interacting atomic pair, which is in agreement with the estimates of Rappé and Bernstein.[1] Also, for the TMA-pyrrole complex, the presence of the dispersion interaction leads to a dramatic change in the optimized structure. Because B3LYP cannot handle properly the dispersion in the calculation, use of the Møller−Plesset second-order perturbation or other sophisticated methods should be considered in computational studies of cation-π interactions in systems containing nonsymmetric dispersion interacted atomic pairs. The orbital interaction is unimportant in the TMA-aromatic interaction according to the detailed analysis of the molecular orbitals. The TMA-aromatic interactions basically come from the typical cation-π interaction and the dispersion interaction. Because the electron density in the Π_5^6 aromatic system of pyrrole is larger than that in the Π_6^6 system of benzene, the π electron cloud on pyrrole is more easily polarized under the influence of cations, which may lead to a relatively stronger cation-π interaction in the TMA-pyrrole complex than in the TMA-benzene complex.

Introduction

In recent years, there has been increasing interest in the interaction of cations with aromatic molecules, the "cation-π interaction", in biological systems.[2,3] This interaction is strong enough to play a significant role in biomolecular recognition, e.g., protein folding and stability, and interactions of drugs with their receptors and enzymes with their substrates.[4−9] Such interactions have been shown to be of particular importance in the interaction of the neurotransmitter acetylcholine (ACh) with ACh receptors and with the synaptic enzyme acetylcholinesterase (AChE), in which the interaction of the quaternary ammonium group with aromatic residues plays an important role, and in the functioning of potassium channels. Specifically, determination of the X-ray structure of *Torpedo californica* AChE (*Tc*AChE) by Sussman et al.[10] showed that a narrow gorge leading to the active site is lined with 14 conserved aromatic residues which play an important role in facilitating substrate and product traffic to and from the active site, and in the formation of the enzyme−substrate complex. In addition, conserved aromatic residues are important for the function of potassium channels.[11] Several experiments by French et al.[12] showed that the normal turn-off of the conductance of K^+ ion channels is associated with quaternary ammonium(QA) binding, and the binding affinity between QA and K^+ channels also involves cation-π interaction. A number of ab initio computations have been performed on TMA-aromatic interactions to obtain a deeper understanding of the physicochemical nature of cation-π interactions in general.[13−15] The dominating factors in cation-π systems have been proposed to be the charge-quadrupole and charge-polarizability interactions.[5] However, Kim et al.[14] suggested that an orbital interaction might be involved in the stabilization of the TMA-benzene complex. But the energy argument used by them to support the presence of the orbital interaction is not totally convincing. In their estimation, the total electrostatic interaction energy amounts to −10.9 kcal·mol^{-1}, which is about 0.8 kcal·mol^{-1} less than the total interaction of the complex without BSSE, and 2.2 kcal·mol^{-1} more than that with BSSE. Considering that the BSSE can be as large as 3 kcal·mol^{-1} in their calculation, one can attribute the energy difference between the total binding

* To whom correspondence should be addressed. Tel: +86-21-64311833 ext. 222. Fax: +86-21-64370269. E-mail: hljiang@mail.shcnc.ac.cn or jiang@iris3.simm.ac.cn.

[†] Center for Drug Discovery & Design, State Key Laboratory of Drug Research, Shanghai Institute of Materia Medica, Shanghai Institutes for Biological Sciences, Chinese Academy of Sciences.

[‡] Chemical Process & Biotechnology Department, Singapore Polytechnic.

[§] Department of Neurobiology, Weizmann Institute of Science.

[||] Department of Structural Biology, Weizmann Institute of Science.

10.1021/jp003098c CCC: $20.00
Published on Web 05/10/2001

energy and the total electrostatic energy to the uncertainty regarding the value of the BSSE. This naturally raises the question whether such an orbital interaction really does exist, and if indeed it does, what is its role?

The chemical nature of the aromatic system has an important effect on the cation-π interaction, especially the presence of a nitrogen atom in the aromatic ring. According to the optimized structure of TMA-benzene obtained by Kim et al.,[14] this complex has C_{3V} symmetry. When the benzene is replaced by pyrrole, the TMA-pyrrole complex loses this symmetry as shown in the study by Pullman et al.[15] Because the pyrrole ring structure is a component of the indole side chain of tryptophan, and the cation-tryptophan interaction is common in biorecognition,[6] it is certainly important to characterize the influence of the heteroatom on the cation-π interaction.

A detailed theoretical comparison of the TMA-benzene and TMA-pyrrole complexes has been performed in order to address the issues raised above. Although these systems have been studied both by Pullman and co-workers[13,15] and by Kim et al.,[14] the physical basis for the geometrical difference between the TMA-benzene and TMA-pyrrole complexes is not well understood, and there is no definitive evidence for or against the existence of an orbital interaction between TMA and benzene. In the following, a physical basis for the loss of symmetry in the TMA-pyrrole complex will be proposed, based on calculations using both the density functional theory (DFT) and Møller−Plesset second-order perturbation (MP2) approaches. Furthermore, possible orbital interaction between TMA and both benzene and pyrrole will be examined.

Computational Methods

Local minima of the TMA-aromatic-ring complexes were fully optimized using both the density-functional theory (B3LYP exchange-correlation functional)[16−18] and the Møller−Plesset second-order perturbation method (MP2).[19−22] Vibrational frequency calculations were then carried out for each optimized structure to verify that it is a local minimum on the potential energy surface. The basis sets used in the optimizations range from the standard valence double-ζ augmented with d and p-like polarization functions on non-hydrogen and hydrogen atoms, respectively (6-31G(d,p)), to the valence triple-ζ plus polarization (6-311G(d,p)), to ensure a correct description of the complex system. Diffuse functions were also added to non-hydrogen atoms to allow orbitals to occupy a larger region of space, to predict more reliable geometric parameters and interaction energies. The calculated interaction energies were corrected for basis set superposition error (BSSE) by means of the counterpoise correction.[23]

All quantum chemistry calculations were carried out with Gaussian 98 software[24] on a Power Challenge R-10000 workstation.

Results and Discussion

TMA-Pyrrole Complex. *Molecular Structure.* Because the initial structure may influence the final optimized local minimum, three different structures of the TMA-pyrrole complex were chosen as starting structures for optimization. The initial structures used were (a) one N−C bond of TMA oriented toward the pyrrole ring, (b) two N−C bonds of TMA oriented toward it, and (c) three N−C bonds of TMA directed toward it.

At the DFT level, all three initial structures converged toward two conformers, in which the three C−N bonds point toward the aromatic ring. The optimized geometries are depicted in Figure 1, along with the important parameters. The vertical projections of the complex are also presented in Figure 1 in order to give a clear view. In Figure 1(a), the projection of one C−N bond staggers the N−H of the pyrrole; hence, this structure will be called the staggered form; the other optimized configuration will then be referred to as the eclipsed form (Figure 1(b)). Vibrational frequency analysis of these two optimized

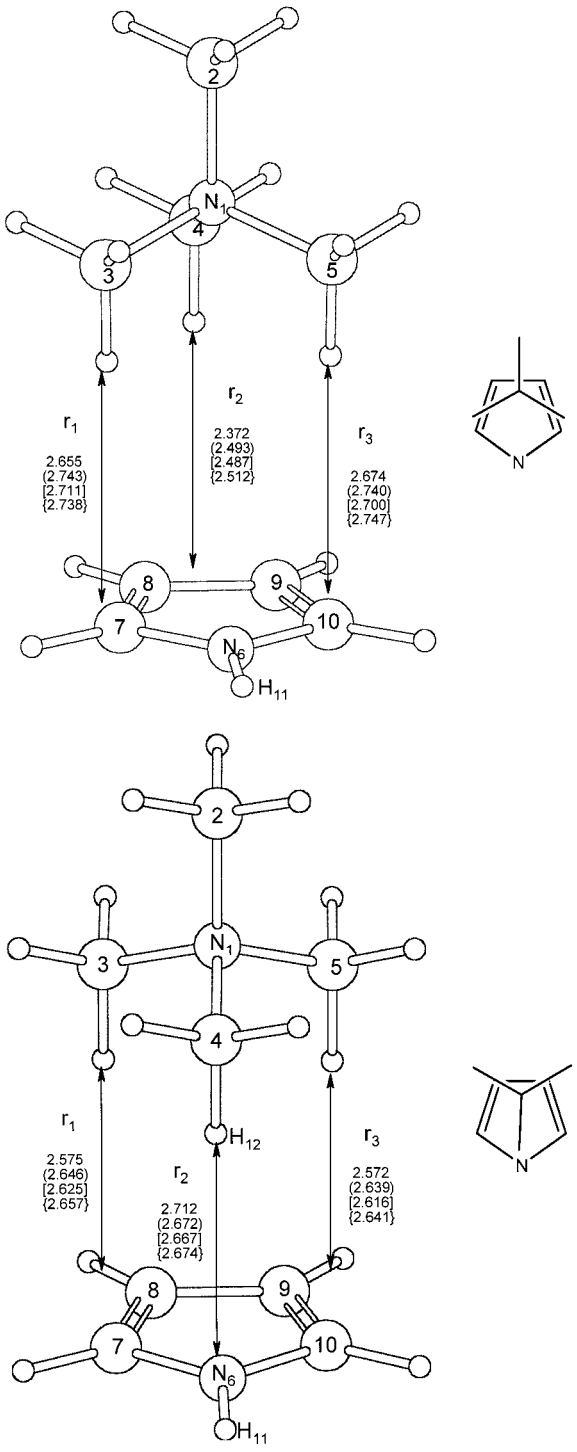

Figure 1. Optimized structures, geometric parameters and vertical view for the TMA-pyrrole complex obtained by the B3LYP method. H atoms are omitted in the vertical view. r_1, r_2, and r_3 are the distances in Å between H atoms of TMA and the plane formed by N_6, C_8, and C_9. Unbracketed data are the B3LYP/6-31G(d,p) results; data in parentheses are the B3LYP/6-31+G(d,p) results; data in brackets are the B3LYP/6-311G(d,p) results, and those in curly brackets are the B3LYP/6-311+G(d,p) results. (**a**) Staggered form; (**b**) Eclipsed form.

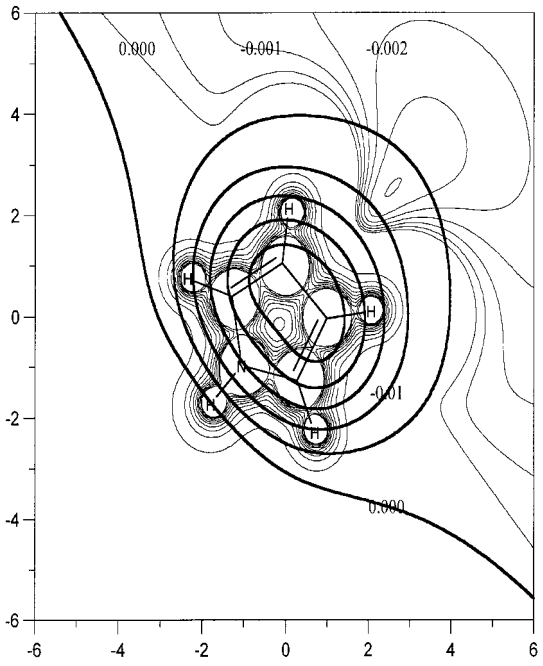

Figure 2. Electrostatic potential map of pyrrole calculated by the B3LYP/6-311+G(d,p) method. The contour spacing is 0.1 Å for the positive part and 0.0005 Å for the negative part. The thin line represents the map in the plane of the pyrrole ring. The thick line represents the ESP 2.5 Å above the pyrrole ring. The contour spacing is 0.005 Å. The units along the two axes are in Å.

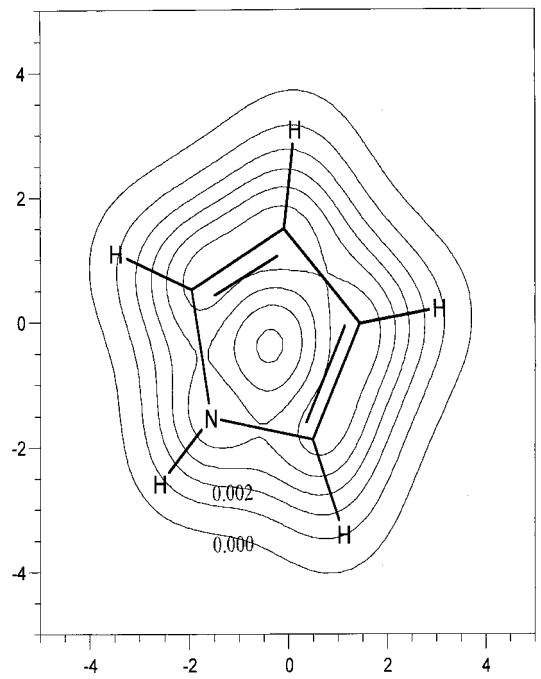

Figure 3. Electronic density map 1.5 Å above the pyrrole produced by the B3LYP/6-311+G(d,p) method. The contour spacing is 0.001 Å. The units along the two axes are in Å.

structures showed that both are true minima on the potential energy surface.

It is clear from Figure 1 that no significant geometric change is observed for the different basis sets used, except for the distances between the three H atoms of TMA pointing toward the pyrrole ring, and the plane of the ring itself (r_1, r_2, and r_3). For the staggered form, the addition of diffuse functions to the basis sets leads to increases of about 0.1 Å in r_1, r_2, and r_3 at the B3LYP/6-31G(d,p) level and of 0.03 Å at the B3LYP/6-311G(d,p) level. The increases for the eclipsed form are ~0.07 Å for r_1 and r_3 with the 6-31G(d,p) basis set, and ~0.03 Å with 6-311G(d,p). A small decrease in r_2 is observed in the eclipsed form as shown in Figure 1b. The dihedral angle $H_{11}-N_6-N_1-C_4$ is affected slightly by the basis sets. In the staggered form, the dihedrals are 177.9° for the 6-31G(d,p) level, 179.4° for the 6-31+G(d,p) level, 173.7° for the 6-311G(d,p) level, and 178.9° for the 6-311+G(d,p) level. The corresponding values for the eclipsed form are 2.5°, 10.1°, 4.6°, and 9.7°, respectively. It is important to notice that the geometric parameters for the conformers are basically the same at the DFT/6-31+G(d,p) and DFT/6-311+G(d,p) levels. The introduction of the diffuse functions into the basis sets seems crucial in the calculations for these weakly bonded systems. Also, the consistence of the geometric parameters obtained with the 6-31+G(d,p) and 6-311+G(d,p) basis sets suggests a reasonable level of basis set completeness.

In both the eclipsed and staggered form, the center of the positive charge of TMA is above the area of the pyrrole ring, at which the electrostatic potential of the ring is the most negative (Figures 1 and 2). In the staggered form, the distances between the pyrrole plane and the hydrogen atoms pointing to the pyrrole are found to be ~2.74 Å for r_1 and r_3, and 2.51 Å for r_2 using the B3LYP/6-311+G(d,p) data. The corresponding values in the eclipsed form are ~2.65 and 2.67 Å, respectively. The slightly shorter r_2 value in the staggered form, and the slightly longer r_2 value in the eclipsed form suggest that there is little repulsion between the H of the methyl group and the aromatic ring. Although in the eclipsed form the $C_4-H_{12}-N_6$ angle is about 165°, and the $H_{12}-N_6$ distance is about 2.7 Å, suggesting existence of a hydrogen-bond, this cannot be a conventional H-bond because there is no lone pair on N_6 in the putative bonding direction. The ESP map in Figure 2 demonstrates that the area above N_6 is not as negative as that over the region of the C−C bond facing it in the pyrrole ring. However, the electronic density map (Figure 3) indicates that the density above the middle of the C−N bond is larger than that above the N atom. Thus, neither ESP nor the electronic density favor the perfect eclipsed form.

The optimized DFT structures were re-optimized at the MP2 level. It is interesting that both conformers converged to the eclipsed form (Figure 4). In contrast to the DFT result, the projection of the positive charge of TMA onto the MP2 prediction is outside the aromatic ring. However, the charge center is not far from the most negative area in the ESP map of pyrrole (Figure 5). It is important to notice that one of the hydrogen atoms of the methyl group points toward the center of the pyrrole ring.

As compared to the structure obtained using B3LYP, the optimized structure at the MP2 level is characterized by a shorter TMA-pyrrole distance. The hydrogen−pyrrole plane distances range from 2.36 to 2.49 Å, about 0.2 Å shorter than the B3LYP predictions, suggesting stronger cation−π interactions. The dihedral angle $H_{11}-N_6-N_1-C_4$ is sensitive to the level of theory, varying from 21.4° (6-311G(d,p)) to 36.5° (6-31G(d,p)). Again, the inclusion of diffuse functions in the calculation is important because their introduction results in lengthening of the hydrogen-pyrrole plane distances by 0.05−0.1 Å.

The quantum chemistry calculation shows that the hydrogen atoms of the pyrrole ring bend out of the plane away from the TMA moiety. The out-of-plane angles range from 2 to 7°. This phenomenon may be associated with the repulsion between the TMA and these hydrogens.

Energetic Properties. The energy characteristics of the TMA-pyrrole complex determined by the B3LYP and the MP2

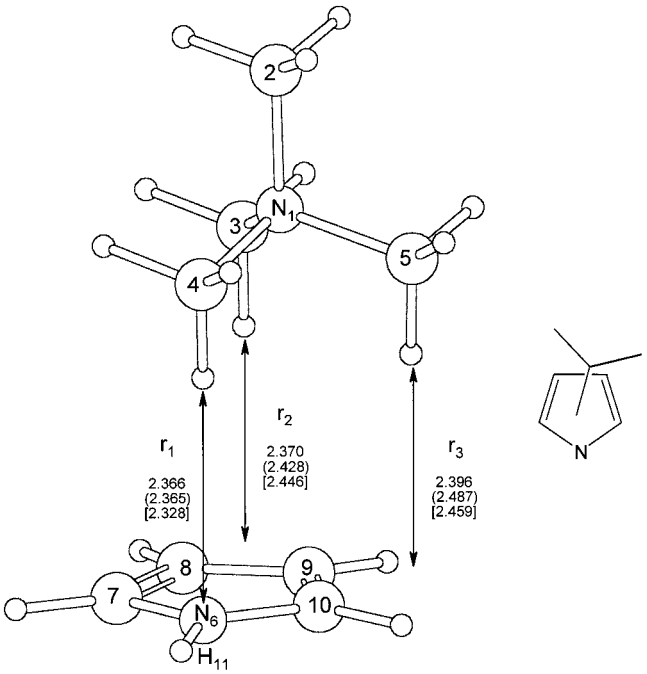

Figure 4. Optimized structures, geometric parameters and vertical view of the TMA-pyrrole complex obtained by the MP2 method. Bond lengths and distances are in Å. H atoms are omitted in the vertical view. r_1, r_2, and r_3 are the distances between H atoms of TMA and the plane formed by N_6, C_8, and C_9. Unbracketed data are the MP2/6-31G(d,p) results; data in parentheses are the MP2/6-31+G(d,p) results, and those in brackets are the MP2/6-311G(d,p) results.

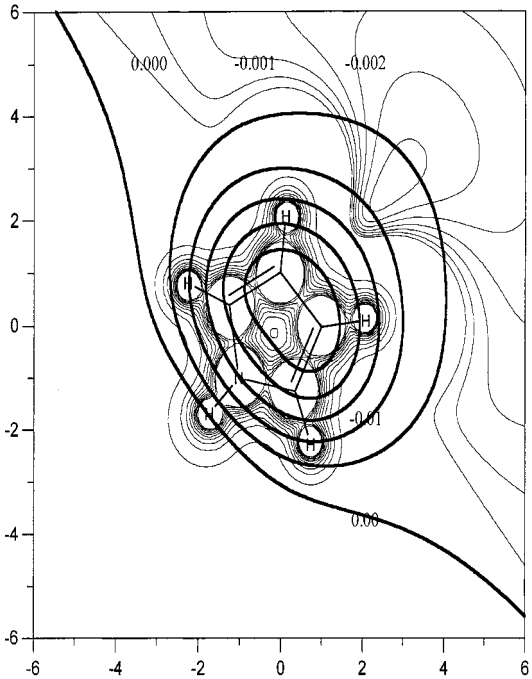

Figure 5. Electrostatic potential map of pyrrole obtained by the MP2/6-31+G(d,p) method. The thin line represents the map in the plane of the pyrrole ring. The contour spacing is 0.1 Å for the positive part and 0.0005 Å for the negative part. The thick line represents the ESP 2.5 Å above the pyrrole ring. The contour spacing is 0.005 Å. The units along the two axes are in Å.

methods are summarized in Table 1. All the B3LYP calculations with the 6-31G(d,p), 6-31+G(d,p), 6-311G(d,p), and 6-311+G(d,p) basis sets give similar values of the BSSE corrected binding energy. The binding energy of the staggered form is about 0.2 kcal·mol^{-1} lower than that of the eclipsed form. Using a triple-ζ plus polarization basis set, including diffuse functions, appears to ensure the reliability of the energetics calculated for the TMA-pyrrole system. This is corroborated by the converged BSSE corrections and by the consistent binding energies predicted with different basis sets (diffuse functions included). The total BSSEs at the B3LYP/6-311+G(d,p) level of theory are as low as 0.13 and 0.35 kcal·mol^{-1}, respectively, for the two conformers of TMA-pyrrole. The BSSEs at the B3LYP/6-31+G(d,p) level are estimated to be 0.30 and 0.43 kcal·mol^{-1}, respectively, for the two conformers, in both cases about 0.2 kcal·mol^{-1} higher than those with 6-311+G(d,p). The consistency of the binding energies at the B3LYP/6-311+G(d,p) and B3LYP/6-31+G(d,p) levels demonstrates the importance of the diffuse functions in the computational studies of weakly bonded complexes.

At the MP2/6-31G(d,p) level, the uncorrected and corrected binding energies of the complex are −13.52 and −10.34 kcal·mol^{-1}, respectively. The BSSE correction is 3.19 kcal·mol^{-1}, suggesting that the basis sets might not be complete. The calculations with 6-311G(d,p) and 6-31+G(d,p) basis sets also exhibit relatively large BSSEs, 2.94 and 2.66 kcal·mol^{-1}, respectively. After the BSSE correction, the binding energies of the complex are −10.41 kcal·mol^{-1} at the MP2/6-311G(d,p) level, and −10.02 kcal·mol^{-1} at the MP2/6-31+G(d,p) level. The larger BSSE suggests that there is a problem of basis set incompleteness associated with the MP2 calculation. More complete basis sets should be used in order to reach the MP2 limit. However, the consistency of the binding energies predicted with different basis sets in this study suggests that use of more sophisticated basis sets in the MP2 calculation will not substantially affect our conclusions.

In agreement with the structural analysis, the binding energy predicted at the MP2 level is larger than that predicted by the B3LYP approach. Upon enlarging the basis set from 6-31G(d,p) to 6-311G(d,p), the binding energy differences (between B3LYP and MP2) are about 2.5 kcal·mol^{-1}. This can be attributed mainly to dispersion interactions which are better described at the MP2 level than by most DFT methods.[1,25,26] The present results are consistent with the estimate of Rappé and Bernstein,[1] according to which the dispersion interaction is roughly 0.5 kcal·mol^{-1} for each first-row interacting atomic pair. In the MP2 optimized structure, there are 5 atomic pairs in direct interaction, as shown in Figure 4, resulting in an estimated dispersion interaction in the system of about 2.5 kcal·mol^{-1}, nearly identical to the binding energy difference between the DFT and the MP2 predictions. Because the dispersion interaction contributes about 25% of the total binding energy, dispersion is expected to have important effects in the TMA-pyrrole complex. Clearly, the shifting away of the positive charge center from the most negative area has been compensated for by the better dispersion interaction in the MP2 optimized structure (Figure 4). The dihedral angle ($H_{11}-N_6-N_1-C_4$) of 30° derived from MP2 optimization is the result of the balance between the dispersion interaction and the electrostatic interaction. The absence of the staggered form at the MP2 level could be interpreted as there being no suitable position for a better dispersion interaction. The shorter distance between TMA and pyrrole may be attributed to dispersion interactions in the MP2 calculation.

TMA-Benzene Complex. *Molecular Structure.* The optimized geometric parameters are depicted in Figure 6. No appreciable differences are observed from previously published results,[13−15] which supports our computational approach. Because the dispersion interactions are not fully taken into account

TABLE 1: Energy Properties of the TMA-pyrrole and TMA-benzene Complexes Evaluated by the B3LYP Method and the MP2 Method

		TMA-pyrrole complex						
		E/hartree			ΔE	BSSE/kcal·mol^{-1}		ΔE^{BSSE}
		TMA	pyrrole	complex	(kcal·mol^{-1})	TMA	pyrrole	(kcal·mol^{-1})
staggered form	B3LYP/6-31G(d,p)	−214.181 286 9	−210.176 337 3	−424.373 693 1	−10.08	0.0085	1.3833	−8.69
	B3LYP/6-31+G(d,p)	−214.183 014 8	−210.188 173 4	−424.383 642 2	−7.82	0.1435	0.1558	−7.52
	B3LYP/6-311G(d,p)	−214.222 671 8	−210.226 079 2	−424.462 685 7	−8.74	0.0521	0.6176	−8.07
	B3LYP/6-311+G(d,p)	−214.223 195 1	−210.230 524 5	−424.466 141 0	−7.79	0.0462	0.0879	−7.66
elipsed form	B3LYP/6-31G(d,p)			−424.373 302 8	−9.84	0.0742	1.3116	−8.45
	B3LYP/6-31+G(d,p)			−424.383 588 3	−7.78	0.2493	0.1842	−7.35
	B3LYP/6-311G(d,p)			−424.462 581 0	−8.68	0.0567	0.7932	−7.83
	B3LYP/6-311+G(d,p)			−424.466 085 9	−7.76	0.0827	0.2728	−7.40
	MP2/6-31G(d,p)	−213.468 551 1	−209.522 623 7	−423.012 727 2	−13.52	0.4623	2.7212	−10.34
	MP2/6-31+G(d,p)	−213.473 329 1	−209.537 683 3	−423.031 662 1	−12.96	0.9844	1.9580	−10.02
	MP2/6-311G(d,p)	−213.538 289 0	−209.593 745 4	−423.153 629 0	−13.55	0.4791	2.1829	−10.41

	TMA-benzene complex							
	E/hartree			ΔE		BSSE/kcal·mol^{-1}		ΔE^{BSSE}
	TMA	benzene	complex	(kcal·mol^{-1})		TMA	benzene	(kcal·mol^{-1})
B3LYP/6-31G(d,p)	−214.181 286 9	−232.258 214 1	−446.451 504 1	−7.53		0.0945	1.2530	−6.18
B3LYP/6-31+G(d,p)// B3LYP/6-31G(d,p)	−214.182 912 8	−232.268 367 1	−446.460 427 3	−5.74		0.0985	0.2256	−5.42
B3LYP/6-311G(d,p)	−214.222 671 8	−232.308 549 9	−446.541 383 4	−6.38		0.0771	0.4212	−5.88
B3LYP/6-311+G(d,p)// B3LYP/6-311G(d,p)	−214.223 026 6	−232.311 199 3	−446.543 695 8	−5.94		0.0670	0.3452	−5.53
MP2/6-31G(d,p)	−213.468 551 1	−231.505 390 7	−444.991 593 8	−11.08	−9.53[a]	0.4221	2.2091	−8.45
MP2/6-31+G(d,p)// MP2/6-31G(d,p)	−213.473 320 9	−231.519 123 9	−445.009 312 5	−10.58	−9.4[b]	1.0225	2.0186	−7.54

[a] Uncorrected enthalpy of formation calculated with binding energy of MP2/6-31G(d,p) and thermal energy calculated by HF/6-31G(d,p). [b] Experimental value of enthalpy of formation of TMA-benzene complex. (ref 27).

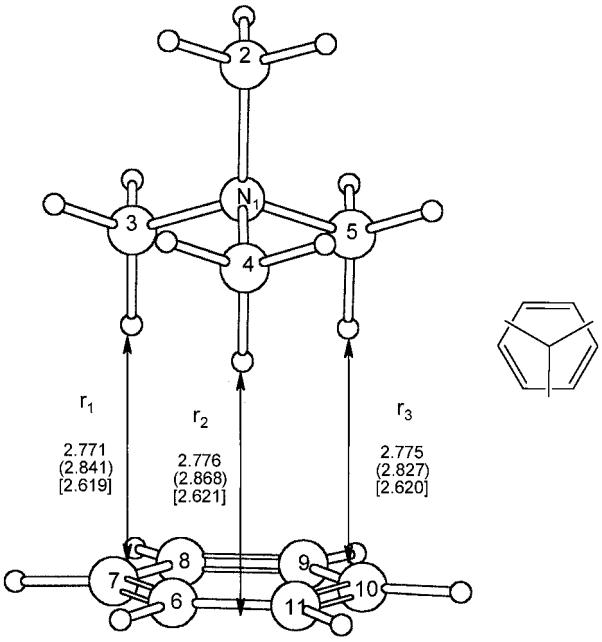

Figure 6. Optimized structures, geometric parameters and vertical view of the TMA-benzene complex obtained by the B3LYP and MP2 methods. Bond lengths and distances are in Å. H atoms are omitted in the vertical view. r_1, r_2, and r_3 are the distances between H atoms of TMA and the plane formed by C_7, C_9, and C_{10}. Unbracketed data are the B3LYP/6-31G(d,p) results; data in parentheses are the B3LYP/6-311G(d,p) results, and those in brackets are the MP2/6-31G(d,p) results.

in the B3LYP approach, the predicted H-benzene plane distances are about 2.78 Å at the DFT level, about 0.16 Å longer than obtained from the MP2 calculations. This is consistent with the results obtained for the TMA-pyrrole system. The interaction between TMA and benzene seems weaker than that between TMA and pyrrole, as can be seen from the TMA-aromatic distances. Both DFT and MP2 methods predicted a longer average H-aromatic distance (by about 0.2 Å) for the TMA-benzene complex than for the TMA-pyrrole complex. Although no symmetry was assumed for the initial geometry, the final structure shows C_{3v} symmetry, as can be seen from Figure 6. In the TMA-benzene complex the C_{3v} symmetric structure permits the highest number of dispersion interactions—the number of interacting atomic pairs being six in this case.

Energetic Properties. The energy properties of the TMA-benzene complex are also listed in Table 1. Diffuse functions are important because adding them to the calculation improves the binding energy by 1 kcal·mol^{-1} (∼10%) at both the B3LYP and the MP2 theoretical levels. As expected, the BSSE is much smaller at the B3LYP level than at the MP2 level. The calculated binding energy at the B3LYP level is ∼5.53 kcal·mol^{-1}, about 1.9 kcal·mol^{-1} smaller than the corresponding value for the TMA-pyrrole complex. This relatively weak binding energy for the TMA-benzene complex is in agreement with the longer TMA-benzene distance. Because the dispersion interactions are not properly accounted for in the DFT calculation, the binding energy by the B3LYP approach is expected be underestimated. The binding energy (ΔE) calculated for the MP2/6-31G(d,p) level is −11.08 kcal/mol (Table 1), very close to the result of Kim et al.[14] calculated by MP2/6-311+G(d,p) (−11.72 kcal/mol). The BSSE-corrected binding energy for the MP2/6-31G(d,p) level is −8.45 kcal/mol, in agreement with the value of −8.67 kcal/mol calculated previously, at the MP2/6-311+G(d,p) reference geometry.[14] The enthalpy of association of the TMA-benzene complex calculated from the binding energy at the MP2/6-31G(d,p) level and the rigid rotor-harmonic oscillator thermal correction at the HF/6-31G(d,p) level is −9.53 kcal·mol^{-1}, which is in very good agreement with the experimental value, −9.4 kcal·mol^{-1}, obtained by Meot-Ner and Deakyne.[27] All these similar values further support the reliability of our computational approaches for TMA-benzene, and by analogy, for TMA-pyrrole, although no comparable experimental

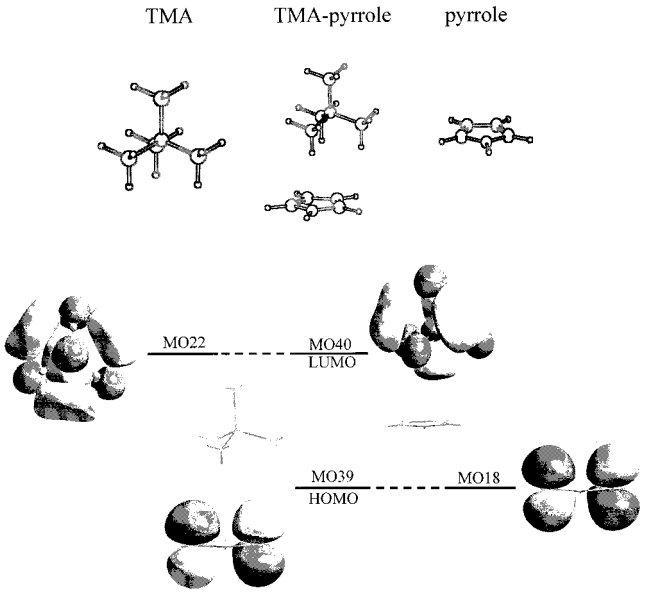

Figure 7. Frontier orbitals of the TMA-pyrrole complex along with the relative molecular orbitals of TMA and pyrrole. The maps of orbitals were obtained at the MP2/6-31+G(d,p) level. The isosurface value of TMA and pyrrole is 0.1, and that of complex is 0.08. It is clear that the LUMO of the complex is basically the orbital of TMA, and the HOMO of the complex is virtually the orbital of pyrrole, implying no orbital interaction between TMA and pyrrole in this system.

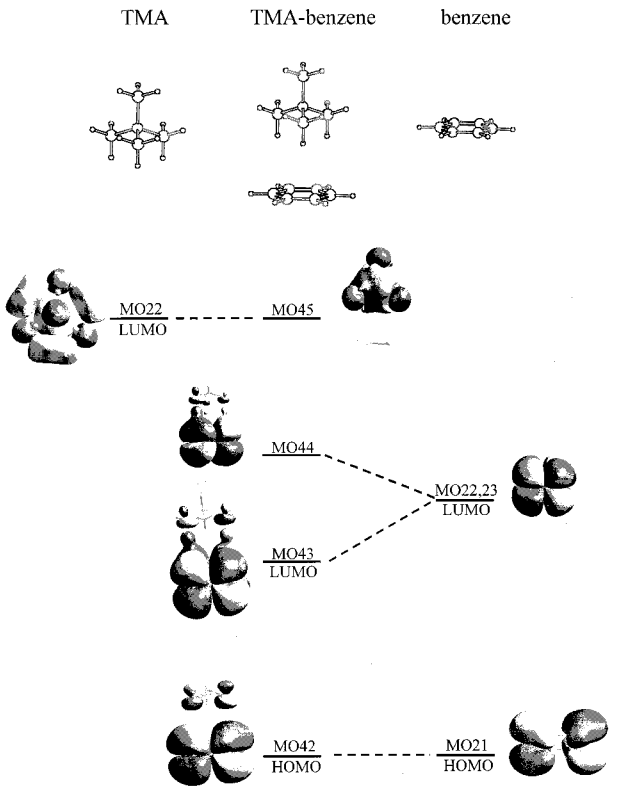

Figure 8. Frontier orbitals of the TMA-benzene complex along with the relative molecular orbitals of TMA and pyrrole. The maps of orbitals were obtained at the MP2/6-31G(d,p) level. The isosurface value of TMA and pyrrole is 0.1, and that of the complex is 0.08. Although there is a splitting of the degenerate π orbitals of benzene under the influence of TMA, the HOMO is basically the HOMO of benzene. The occupied orbitals of the TMA-benzene complex do not show an orbital interaction between TMA and benzene.

results are available for the latter system. As for the TMA-pyrrole complex, the dispersion energy for the TMA-benzene system is increased to 2.1 kcal·mol^{-1}, about 27% of the total binding energy. Because six atomic pairs are involved in the dispersion interaction in this system, the average dispersion energy amounts to ~0.35 kcal·mol^{-1} per atomic pair. Considering that the distance between TMA and benzene is longer than between TMA and pyrrole, such a dispersion energy of 0.35 kcal·mol^{-1} per pair is consistent with the estimate of 0.5 kcal·mol^{-1} per pair in the TMA-pyrrole system.

As discussed above, the interaction of TMA with benzene is weaker than with pyrrole, even though one more atomic pair interacts through dispersion in the TMA-benzene system. The stronger binding between the cation and the aromatic ring in the TMA-pyrrole system may be reasonably attributed to the presence of the N atom in the aromatic ring. The electron density in the Π_5^6 aromatic system of pyrrole is larger than that in the Π_6^6 system of benzene. Consequently, the π electron cloud on pyrrole is more easily polarized under the influence of a cation, resulting in a relatively strong binding interaction because cation-π binding strength is related to the polarizability of the aromatic ring.[5]

Molecular Orbital Analysis. In the TMA-benzene complex, the π electrons in the benzene ring are assumed to interact with the σ^* orbitals of the C−H bonds in TMA.[14] If this were also true for the TMA-pyrrole complex, a small elongation of the C−H bond directed toward the pyrrole ring should be noticed. However, we have not observed such an elongation, indicating that there is no interaction between the σ^*_{C-H} in TMA and the π orbital. This conclusion is further buttressed by the molecular orbital diagram depicted in Figure 7. The HOMO of pyrrole and σ-like contribution of C−H antibonding orbitals that orient perpendicularly to the pyrrole plane constitute the HOMO of the complex. It is clear that the HOMO of the complex is mainly formed by the HOMO of pyrrole. The LUMO is basically the LUMO of TMA. We also find that three orbitals below the HOMO are the π orbitals of pyrrole.

TABLE 2: Orbital Compositions Calculated Using MP2/6-31G(d,p) Method of TMA-benzene

	41MO	42MO	43MO	44MO	45MO
benzene	96.0%	96.1%	99.4%	87.5%	9.7%
TMA	4.0%	3.9%	0.6%	12.5%	90.3%

This conclusion is consistent with our expectations. The distances between C atoms pointing toward the pyrrole and the pyrrole plane are >3.5 Å, and those between H atoms of TMA and aromatic plane are >2.4 Å. It is difficult to form orbital interactions for the H atoms. Moreover, the symmetry of the σ^* style C−H orbital does not match that of the π orbital of pyrrole, i.e., symmetry considerations preclude interaction between these two orbitals.

To examine the importance of the orbital interaction in the TMA-benzene complex, we analyzed the orbitals in detail. Figure 8 presents the frontier orbital diagrams of the TMA-benzene complex. Under the influence of TMA, the degenerate π orbital MO22 and MO23 in benzene splits, becoming the main contributor to MO43 and MO44 in the TMA-benzene system. The monomers' contributions to the frontier orbitals of the complex are listed in Table 2. It is obvious that the HOMO and the LUMO are composed of p orbitals of carbon atoms of benzene mainly, which leads to a large percentage contribution from benzene. The LUMO contains 99.4% benzene π orbital character, so it is a typical example of a nonbonding orbital. The HOMO also shows the nonbonding characters. The benzene orbital contributes 96.1% to the HOMO of the complex. Although two σ^* orbitals of C−H in TMA has the appropriate

orbital orientation to combine with the π orbital of benzene, the calculation at the B3LYP/6−311g(d,p) level shows that the distances between H and the benzene plane are about 2.8 Å (2.6 Å at the MP2 level). We can conclude that there is little orbital interaction between TMA and benzene. Therefore, we can attribute most of the binding energy of the complex to dispersion and electrostatic interaction, which is in agreement with the concept of the cation-π interaction proposed by Dougherty.[5]

Conclusions

We have presented a comprehensive theoretical study of cation-aromatic interactions of TMA with pyrrole and benzene by means of the B3LYP density-functional method, and by the ab initio MP2 method using various basis sets. We find that it is important to add diffuse functions to the basis set in computational studies of weakly bonded cation-aromatic complexes. Adding the diffuse functions in the calculation decreases the binding energy by ∼10% for the TMA-aromatic systems. Dispersion interactions play an important role in the TMA-aromatic system, ∼0.5 kcal·mol^{-1} per interacting atomic pair, in agreement with the estimation by Rappé and Bernstein.[1] For some complexes, e.g., TMA-pyrrole in the present study, the dispersion interactions may lead to dramatic changes in structure. Because most DFT methods cannot properly handle dispersion interactions, MP2, or other correlated ab initio methods should be considered in computational studies of cation-π interactions in systems containing nonsymmetric dispersion interaction atomic pairs. The orbital interaction is unimportant in the TMA-aromatic interaction, which basically involves cation-π and dispersion interactions. Because the electron density in the Π_5^6 aromatic system of pyrrole is larger than in the Π_6^6 system of benzene, the π electron cloud on pyrrole is more easily polarized under the influence of cations, thus increasing the binding energy.

Acknowledgments. We gratefully acknowledge financial support from the National Natural Science Foundation of China (Grant No. 29725203), the "863" High-Tech Program of China (Grant No. 863-103-04-01), the State Key Program of Basic Research of China (Grant No. 1998051115). This work was also supported by the U.S. Army Medical and Materiel Command under Contract No. DAMD17-97-2-7022, the EU Fourth Framework Program in Biotechnology, the Kimmelman Center for Biomolecular Structure and Assembly (Rehovot, Israel), and the Dana Foundation. We thank Dr. Jan M. L. Martin for valuable discussions and for critical reading of the manuscript. I. S. is the Bernstein-Mason Professor of Neurochemistry. The quantum chemistry calculations were performed on Power Challenge R10000 at The Network Information Center, Chinese Academy of Sciences, Beijing, P. R. China.

References and Notes

(1) Rappé, A. K.; Bernstein, E. R. *J. Phys. Chem. A* **2000**, *104*, 6117−6128.
(2) Yellen, G.; Jurman, M. E.; Abramson, T.; MacKinnon, R. *Science* **1991**, *251*, 939−942.
(3) Mecozzi, S.; West, A. P.; Dougherty, D. A. *Proc. Natl. Acad. Sci. U.S.A.* **1996**, *93*, 10 566−10 571.
(4) Ma, J. C.; Dougherty, D. A. *Chem. Rev.* **1997**, *97*, 1303−1324.
(5) Dougherty, D. A. *Science* **1996**, *271*, 163−168.
(6) Gallivan, J. P.; Dougherty, D. A. *Proc. Natl. Acad. Sci. U.S.A.* **1999**, *96*, 9459−9464.
(7) Kumpf, R. A.; Dougherty, D. A. *Science* **1993**, *261*, 1708−1710.
(8) Zhu, W.-L.; Tan, X.-J.; Puah, C. M.; Gu, J.-D.; Jiang, H.-L.; Chen, K.-X.; Felder, C.; Silman, I.; Sussman, J. L. *J. Phys. Chem. A* **2000**, *104*, 9573−9580.
(9) Tan, X. J.; Jiang, H. L.; Zhu, W. L.; Chen, K. X.; Ji, R. Y. *J. Chem. Soc., Perkin Trans. 2* **1999**, *1*, 107−112.
(10) Sussman, J. L.; Harel, M.; Frolow, F.; Oefner, C.; Goldman, A.; Toker, L.; Silman, I. *Science* **1991**, *253*, 872−879.
(11) Sussman, J. L.; Silman, I. *Curr. Opin. Struct. Biol.* **1992**, *2*, 721−729.
(12) French, R. J.; Shoukimas, J. J. *Biophys. J.* **1981**, *34*, 271−291.
(13) Pullman, A.; Berthier, G.; Savinelli, R. *J. Am. Chem. Soc.* **1998**, *120*, 8553−8554.
(14) Kim, K. S.; Lee, J. Y.; Lee, S. J.; Ha, T.-K.; Kim, D. H. *J. Am. Chem. Soc.* **1994**, *116*, 7399−7400.
(15) Pullman, A.; Berthier, G.; Savinelli, R. *J. Comput. Chem.* **1997**, *18*, 2012−2022.
(16) Becke, A. D. *J. Chem. Phys.* **1993**, *98*, 5648−5652.
(17) Lee, D.; Yang, W.; Parr, R. G. *Phys. Rev. B* **1988**, *37*, 785−789.
(18) Miehlich, B.; Savin, A.; Stoll, H.; Preuss, H. *Chem. Phys. Lett.* **1989**, *157*, 200.
(19) Frisch, M. J.; Head-Gordon, M.; Pople, J. A. *Chem. Phys. Lett.* **1990**, *166*, 275.
(20) Head-Gordon, M.; Pople, J. A.; Frisch, M. J. *Chem. Phys. Lett.* **1988**, *153*, 503.
(21) Head-Gordon, M.; Head-Gordon, T. *Chem. Phys. Lett.* **1994**, *220*, 122−128.
(22) Saebø, S.; Almlof, J. *Chem. Phys. Lett.* **1989**, *154*, 83−89.
(23) Boys, S. F.; Bernardi, F. *Mol. Phys.* **1970**, *19*, 553−566.
(24) Frisch, M. J.; Trucks, G. W.; Schlegel, H. B.; Scuseria, G. E.; Robb, M. A.; Cheeseman, J. R.; Zakrzewski, V. G.; Montgomery, J. A.; Stratmann, R. E.; Burant, J. C.; Dapprich, S.; Millam, J. M.; Daniels, A. D.; Kudin, K. N.; Strain, M. C.; Farkas, O.; Tomasi, J.; Barone, V.; Cossi, M.; Cammi, R.; Mennucci, B.; Pomelli, C.; Adamo, C.; Clifford, S.; Ochterski, J.; Petersson, G. A.; Ayala, P. Y.; Cui, Q.; Morokuma, K.; Malick, D. K.; Rabuck, A. D.; Raghavachari, K.; Foresman, J. B.; Cioslowski, J.; Ortiz, J. V.; Stefanov, B. B.; Liu, G.; Liashenko, A.; Piskorz, P.; Komaromi, I.; Gomperts, R.; Martin, R. L.; Fox, D. J.; Keith, T.; Al-Laham, M. A.; Peng, C. Y.; Nanayakkara, A.; Gonzalez, C.; Challacombe, M.; Gill, P. M. W.; Johnson, B. G.; Chen, W.; Wong, M. W.; Andres, J. L.; Head-Gordon, M.; Replogle, E. S.; Pople, J. A. Gaussian 98 (Revision A.7); Gaussian, Inc.: Pittsburgh, PA, 1998.
(25) Ruiz, E.; Salahub, D. R.; Vela, A. *J. Am. Chem. Soc.* **1995**, *117*, 1141−1142.
(26) Hobza, P.; Sponer, J.; Reschel, T. J. *J. Comput. Chem.* **1995**, *16*, 1315.
(27) Meot-Ner(Mautner), M.; Deakyne, C. A. *J. Am. Chem. Soc.* **1985**, *107*, 469−474.